ELSEVIER

Hearing Research 76 (1994) 31–44

HEARING RESEARCH

Spatiotemporal encoding of sound level: Models for normal encoding and recruitment of loudness

Laurel H. Carney

Department of Biomedical Engineering, Boston University, 44 Cummington Street, Boston, MA 02215, USA

(Received 18 August 1993; Revision received 17 January 1994; Accepted 19 January 1994)

Abstract

This study explores the hypothesis that sound level is encoded in the spatiotemporal response patterns of auditory nerve (AN) fibers. The temporal properties of AN fiber responses depend upon sound level due to nonlinearities in the auditory periphery. In particular, the compressive nonlinearity of the inner ear introduces systematic changes in the timing of the responses of AN fibers as a function of level. Changes in single fiber responses that depend upon both sound level and characteristic frequency (CF) result in systematic changes in the spatiotemporal response patterns across populations of AN fibers. This study investigates the changes in the spatiotemporal response patterns as a function of level using a computational model for responses of low-frequency AN fibers. A mechanism that could extract information encoded in this form is coincidence detection across AN fibers of different CFs. This study shows that this mechanism could play a role in encoding of sound level for simple and complex stimuli. The model demonstrates that this encoding scheme would be influenced by auditory pathology that affects the peripheral compressive nonlinearity in a way that is consistent with the phenomenon of recruitment of loudness, which often accompanies sensorineural hearing loss.

Key words: Auditory nerve; Compressive nonlinearity; Intensity coding; Dynamic range; Loudness recruitment; Spatiotemporal patterns

1. Introduction

Auditory encoding of sound level, and the associated perception of loudness, is a phenomenon that is still not well understood. This issue is critical to our understanding of the fundamentals of information encoding and processing in the auditory system. Furthermore, one of the most common and problematic aspects of sensorineural hearing impairment is the resulting change in the perception of loudness. Better understanding of the normal mechanisms for encoding sound level and of how these mechanisms are affected by specific impairments of the auditory system should lead to better strategies for aiding the hearing impaired.

We perceive changes in the loudness of auditory stimuli over the entire range of hearing, which far exceeds the dynamic range of most AN fibers. Many psychophysical and physiological studies have investigated the encoding of sound level (e.g. Hellman, 1974, 1978; Smith and Brachman, 1980a; Evans, 1981; Palmer and Evans, 1982; Smith et al., 1983; Colburn, 1984; Moore et al., 1985; Sachs et al., 1986; Delgutte, 1987; Winslow et al., 1987; Smith, 1988; Viemeister, 1988a,b; Winslow and Sachs, 1988; Winter and Palmer, 1991; May and Sachs, 1992). The two major classes of hypothesized encoding schemes are rate-place coding and temporal coding (timing cues).

Rate-place schemes are based on the changes in average discharge rate of AN fibers as a function of level and the spread of excitation across the population of fibers as SPL is increased. For the majority of AN fibers, the dynamic range of average discharge rate during the sustained response is limited to 20–50 dB (Kiang et al., 1965; Sachs and Abbas, 1974; Evans and Palmer, 1980; Palmer and Evans, 1982). This limited dynamic range constrains the ability of rate mechanisms to explain the wide behavioral dynamic range of humans and other animals. However, physiological evidence for a small number of AN fibers with wide

* Corresponding author. Fax: 617-353-6766.

0378-5955/94/$07.00 © 1994 Elsevier Science B.V. All rights reserved
SSDI 0378-5955(94)00023-J

dynamic ranges, as evidenced by sloping or nonsaturated rate-level functions (e.g. Sachs and Abbas, 1974; Liberman, 1978; Winter et al., 1990; Winter and Palmer, 1991) prevents the rate-place coding scheme from being discounted.

Psychophysicists have explored rate-place schemes for encoding of sound level by trying to limit the amount of temporal information available to the listener. For example, tonal stimuli at high frequencies, for which AN fibers do not phase-lock to the fine structure of the stimulus, should provide minimal temporal cues for level. For high frequency tones, intensity discriminations could presumably be based upon either rate mechanisms that depend heavily upon non-saturating fibers (Delgutte, 1987; Winslow et al., 1987; Viemeister, 1988a,b; Winter and Palmer, 1991), or upon spread of excitation (Delgutte, 1987). Some studies have attempted to mask the spread of excitation cue by presenting the target stimulus in a band-stop noise (e.g. Hellman, 1974, 1978; Palmer and Evans, 1982; Viemeister, 1983; Moore et al., 1985). This masking paradigm, however, introduces potential temporal cues, because high-CF AN fibers phase-lock to the envelope of complex signals (Smith and Brachman, 1980b; Palmer, 1982; Joris and Yin, 1992), and narrowband filtering of noise by the auditory periphery provides amplitude-modulated signals to which AN fibers can phase-lock. The report of temporal correlation between responses to wideband noise of high-CF fibers with neighboring CFs (Young and Sachs, 1989) provides evidence for such temporal patterning.

There are several unsolved problems related to the rate-place scheme for encoding level. If the rates of non-saturating fibers are exploited for encoding of high levels, then the responses of these fibers must be processed separately by the CNS, lest the information that they encode be lost when combined with the higher discharge rates of the more prevalent saturating fibers (Winslow et al., 1987; Yates et al., 1990; Lai et al., 1993). In addition, the presence of non-saturating fibers is reportedly quite rare at CFs below 1.5 kHz (Winter and Palmer, 1991), which motivates further study of cues that the nervous system may use for encoding of level, especially at low frequencies.

The other major class of schemes for encoding sound level involves timing cues (e.g. Evans, 1978, 1981). The most promising scheme based on timing cues focusses on the relative strength of synchronization of phase-locked responses to different components in a complex stimulus (Young and Sachs, 1979; Evans, 1981), yet this scheme cannot explain encoding of level for simple (tonal) stimuli. Although, phase-locking of low-CF AN fibers to the fine structure of a tone is present at all levels to which the fibers respond, strength of phase-locking does not increase monotonically as a function of level. Rather strength of synchronization peaks at relatively low levels and declines slightly as level is increased (Johnson, 1980). Of course, a temporal encoding scheme based upon phase-locking to the fine structure of a tone at CF is limited to low-CF fibers.

This study investigates the encoding of sound level by a combination of place and timing properties of responses, that is, by the spatiotemporal response patterns of AN fibers. Rather than depending upon the strength of phase-locking in the responses of single fibers, the primary feature of the model presented here is that it takes advantage of cues that are present in the patterns of activity across fibers with different CFs. The simultaneous discharge pattern of a population of AN fibers with different CFs is referred to as the spatiotemporal discharge pattern. Systematic changes in the timing of single fiber responses, such as changes in the dominant phase of their phase-locked responses, result in systematic changes in the spatiotemporal discharge patterns.

The compressive nonlinearity of the inner ear results in changes in the bandwidth of tuning in the periphery as a function of sound level (e.g. Rhode, 1971; Robles et al., 1986; reviewed by Patuzzi and Robertson, 1988). This study focusses on changes in the spatiotemporal discharge patterns as a function of level that are introduced by the compressive nonlinearity. Systematic changes in the peripheral bandwidth, and the associated changes in the phase properties of the peripheral filters, can explain empirically demonstrated changes in the temporal response properties of low-frequency AN fibers to simple (Anderson et al., 1971) and complex (Carney and Yin, 1988; Horst et al., 1990) stimuli as a function of level. Changes in bandwidth as a function of level have also been demonstrated in psychophysical estimates of peripheral tuning (Pick, 1980; Moore and Glasberg, 1987).

The spatiotemporal cue for sound level that is introduced by the compressive nonlinearity can be decoded by a coincidence-detecting cell that receives AN inputs having different CFs. Such spatiotemporal processing could be performed at any level of the auditory brainstem where cells receive converging inputs from lower levels. There is physiological evidence that several types of cells in the anteroventral cochlear nucleus (AVCN) that receive convergent AN inputs are sensitive to the temporal response pattern across the inputs (Carney, 1990).

The encoding of sound level in spatiotemporal patterns of AN fibers that is proposed here depends heavily upon the presence of the compressive nonlinearity in the auditory periphery. This nonlinearity has been associated with the active process of the inner ear, which is notably susceptible to exposure to noise trauma and damage due to ototoxic drugs (e.g. Patuzzi et al., 1989; Ruggero and Rich, 1991; Ruggero et al., 1992, 1993). Damage to the active process, and thus to

the compressive nonlinearity, has been qualitatively associated with sensorineural hearing loss and with the phenomenon of recruitment of loudness (e.g. Moore, 1989). Recruitment of loudness is the abnormal growth of loudness that often accompanies sensorineural hearing loss of cochlear etiology (e.g. Fowler, 1936; Jerger, 1962; Hood, 1969, 1977). The AN fiber and coincidence detection models presented here allow the direct simulation of the consequences of the loss of the compressive nonlinearity on the proposed scheme for encoding of level. Removal of the compressive nonlinearity and the associated spatiotemporal cues for level, when coupled with the properties of the coincidence detection mechanism, produces responses that demonstrate a potential neural correlate for recruitment of loudness.

A preliminary version of this study has been presented previously (Carney, 1993b).

2. Methods

The results in this study are based on modelled spatiotemporal response patterns of AN fibers and of postsynaptic cells that act as coincidence detectors. The model for low-frequency AN fiber responses is fully described elsewhere (Carney, 1993a). In brief, the model includes a time-varying peripheral filter followed by a travelling wave delay and models for the inner hair cell (IHC) and IHC-AN synaptic transmission (Fig. 1). The bandwidth of the time-varying filter is controlled by a nonlinear feedback loop that provides the compressive nonlinear behavior of the model. The travelling-wave delay for each AN is determined by its CF, based on empirical AN response properties (Carney and Yin, 1988). The IHC model contains a memoryless saturating nonlinearity and a 2nd-order low-pass filter. The IHC voltage provides the input to a diffusion model similar to that of Westerman and Smith (1988) for release of neurotransmitter at the IHC-AN synapse. Finally, a discharge generator with absolute and relative refractoriness provides discharge times in response to arbitrary stimuli. The most important attribute of the AN model for the purposes of this study is that it simulates the nonlinear temporal properties of AN responses to simple and complex stimuli over a wide range of SPLs.

In this study, the responses of populations of model AN fibers to tones and wideband noise were investigated. The population model was simply a bank of single fiber models that were selected to have particular CFs. The spike times of the model AN fibers provided the inputs for a post-synaptic cell model. The cell model received convergent AN fiber inputs and was sensitive to the temporal coincidence of its inputs (see Fig. 6, below). The model used to simulate the

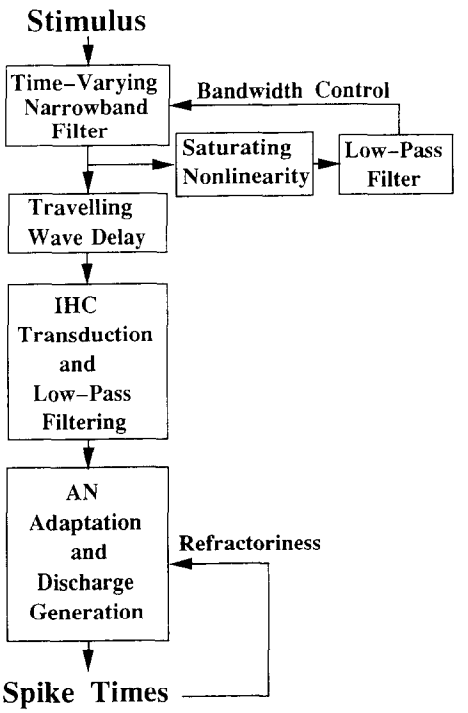

Fig. 1. Simplified schematic diagram of the model for AN fibers. For more details, see Carney 1993a.

postsynaptic neuron was a simple 'shot-noise' model that has been used to investigate responses of globular bushy cells in the anteroventral cochlear nucleus (Carney, 1992; Young et al., 1993; Joris et al., 1994) and principal cells in the medial superior olive (MSO) (Colburn et al., 1990). In this model, each input discharge produces a simplified excitatory post-synaptic potential (EPSP) that is represented by an instantaneous increase in postsynaptic voltage that decays exponentially over time. These EPSPs are simply summated by the postsynaptic cell, and a discharge is produced when the summed inputs reach a set voltage that represents the threshold of the cell. After a discharge of the postsynaptic cell model, the postsynaptic voltage is reset to zero and there is an absolute refractory period of 1 ms during which input discharges are not able to depolarize the cell, simulating after-hyperpolarization.

The initial amplitude of the EPSP and the time constant of its decay were important parameters that determined the sensitivity of the model cell to the temporal coincidence of its inputs. For example, inputs with smaller amplitudes or shorter time courses required a higher degree of temporal coincidence to bring the post-synaptic cell voltage to threshold for discharge. Note that a short duration model 'EPSP' need not indicate a synaptic current of the same duration; rather, the duration of the model EPSP represents the duration of the overall influence of an input discharge upon the postsynaptic cell. For example, in

the AVCN the influence of a synaptic input may be truncated by voltage-sensitive postsynaptic currents that repolarize cells, making it more difficult for separate inputs to temporally summate (Manis and Marx, 1991; Stutman and Carney, 1993).

Two other parameters of the model were important for the mechanism explored in this study. One was the number of AN inputs that converge upon the postsynaptic cell model; the number of inputs as well as their amplitudes and time courses determine the sensitivity of the cell to coincidence and its spontaneous and driven discharge rates. The other parameter of interest was the range of CFs of the input fibers. The spatiotemporal cues that were investigated were present across different CFs. Therefore, the postsynaptic cell received convergent inputs with different CFs and decoded this information on the basis of coincidence detection. A broader range of CFs converging upon a single cell provided a larger absolute change in the degree of coincidence between the responses of different input fibers as a function of SPL.

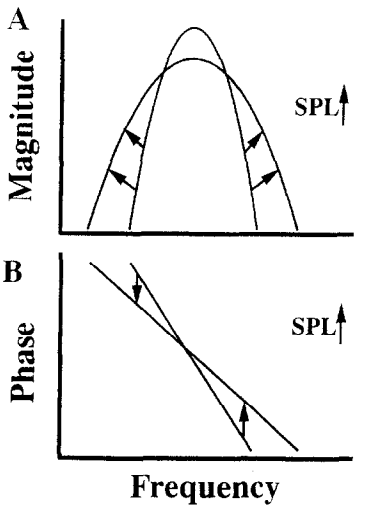

Fig. 2. Schematic illustration of the changes in bandwidth of the peripheral filters as a function of level. Arrows indicate the directions of change in the filter properties as SPL is increased. The broadening of the magnitude bandwidth of the transfer function (A) is accompanied by a change in the slope of the phase of the transfer function (B).

3. Results

The first part of this study involves the changes in timing of AN responses as a function of sound level. In particular, contributions of changes in single fiber responses to changes in the spatiotemporal response patterns are investigated. Then, the properties of a coincidence detection mechanism that receives AN inputs with different CFs is explored.

Responses of model for a single AN fiber

The timing of phase-locked responses of single AN fibers changes as a function of level. The compressive nonlinearity produces a change in bandwidth of the peripheral filters as a function of level, as shown schematically in Fig. 2A. Because the change in the bandwidth of a filter is accompanied by a change in its phase properties (Fig. 2B), the timing of phase-locked low-CF AN responses is directly affected by the compressive nonlinearity.

The influence of the compressive nonlinearity is illustrated in Fig. 3 for the response of a model AN fiber with CF of 500 Hz. The format of the figure is similar to that in Anderson et al. (1971), in which changes in the phase of low-CF AN responses as a function of level were first demonstrated. Fig. 3a shows the response area of the fiber; average discharge rate is plotted as a function of stimulus frequency and SPL. The phase angle of each phase-locked response was computed from its period histogram. Fig. 3b shows these phases plotted with respect to the phase of the response at each frequency at 90 dB SPL. The phases change systematically as a function of level in response to frequencies above and below the CF. This pattern of level-dependent phase can be explained by the changes in the peripheral filter schematized in Fig. 2.

Responses of AN population model

Changes in the spatiotemporal discharge patterns that are a direct result of the nonlinear single-fiber responses are illustrated in the next two figures. The effects of changes in the timing of single fiber responses on the spatiotemporal pattern of a population can be illustrated with a bank of model AN fibers. Fig. 4 shows the responses to a 500-Hz tone of a group of model AN fibers with CFs ranging from 360 to 650 Hz. The amplitude of the response of each model peripheral filter is related to the probability of discharge as a function of time (Fig. 4A,B). The peak trajectories represent the times of greatest discharge probability, and thus provide a representation of the most probable spatiotemporal discharge pattern for this group of fibers. The trajectories of peaks across different CFs clearly change in slope as level is changed from 50 to 70 dB SPL.

The change in the spatiotemporal response patterns as a function of level has an important property: as level is increased, the timing of responses across different frequencies becomes more similar. That is, fibers with different CFs discharge more coincidently as level is increased. This trend is shown in an enlarged plot of the filter bank response to 500 Hz tones at four SPLs (Fig. 5). The slopes of the peak trajectories of the spatiotemporal discharge patterns encode the SPL of the stimulus over the wide dynamic range of the model's compressive nonlinearity, from approximately 30–40

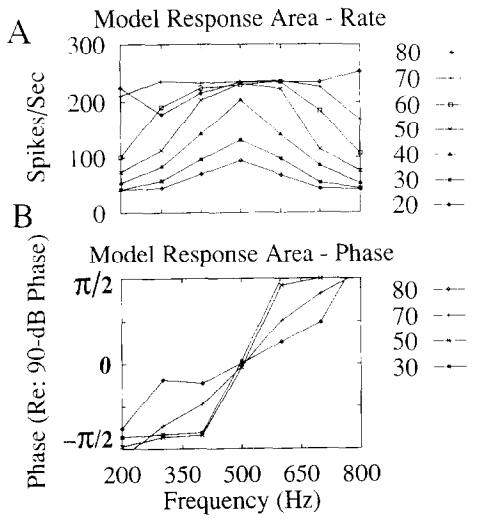

Fig. 3. Iso-level curves (A) and corresponding phase curves (B) for a model AN fiber with CF of 500 Hz. Each point in A represents the average sustained discharge rate in response to 400 repetitions of a 50 ms tone pip presented every 100 ms. Phases are referenced to the phase of the response at 90 dB SPL at each frequency (following the convention of Anderson et al. 1971).

dB SPL to 90–100 dB SPL (Yates et al., 1990; Ruggero, 1992; Ruggero et al., 1992). Furthermore, the phase changes introduced by the compressive nonlinearity are appropriate for decoding by a coincidence detection mechanism that receives inputs from fibers with different CFs: the responses of fibers with different CFs become increasingly coincident as level is increased.

Coincidence-detecting cell model

The method for simulating the response of a coincidence-detecting model cell is illustrated in Fig. 6. Responses of model AN fibers with different CFs to a 500-Hz tone were simulated (Fig. 6a). PST histograms of the responses of each fiber are shown; each fiber phase-locks to the frequency of the input tone, but the phase of the phase-locked responses is determined by the CF of the fiber relative to the stimulus frequency and by the stimulus level. In order to simulate the responses of a coincidence-detecting cell, the AN discharge times are used, on a trial-by-trial basis, as inputs to the model postsynaptic cell. The EPSPs elicited during a single trial are shown schematically in Fig. 6b. Fig. 6c shows the PST histogram for the responses of the postsynaptic model cell to several repetitions of the stimulus.

Rate-level functions of coincidence-detecting model cells were investigated to explore the ability of this mechanism to decode the information about level that is encoded in the spatiotemporal pattern. In Fig. 7, the dotted lines are the rate-level functions for 5 model AN fibers with difference CFs that were inputs to a coincidence detecting cell, and the solid line represents the rate-level function for the model cell. For this illustration, the CFs of the inputs were chosen relatively close to 500 Hz so that all of the inputs saturated at high SPLs in response to the 500 Hz tonal stimulus. Also, the model AN fibers all had high spontaneous rates and flat saturations. The only changes in the AN inputs at levels above 40 dB SPL were the phase

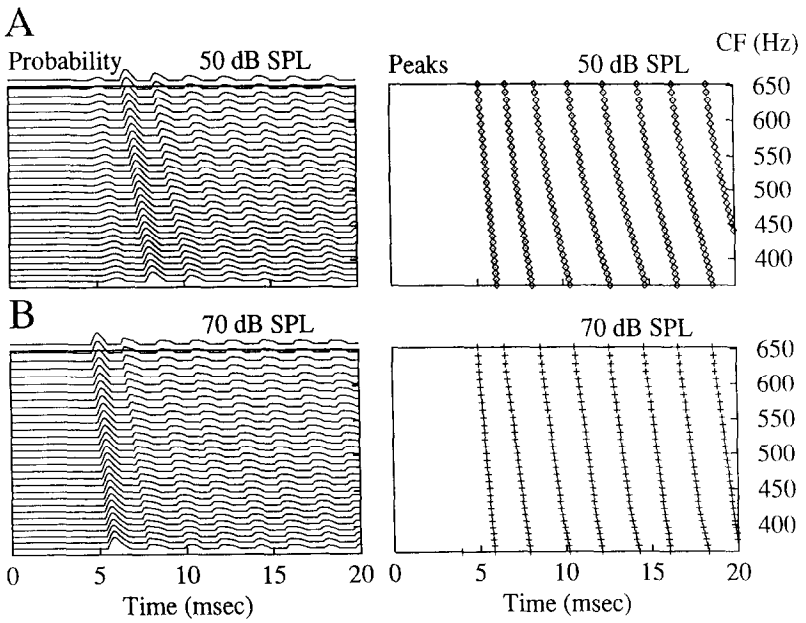

Fig. 4. Responses of a population of model AN fibers to a 500-Hz tone at different SPLs. CFs vary from 360 to 650 Hz. Responses at 50 dB SPL (A) and 70 dB SPL (B). Left: Each curve represents the probability of firing as a function of time after the onset of the tone. Right: Spatio-temporal response patterns are estimated by picking the peaks in the probability curves.

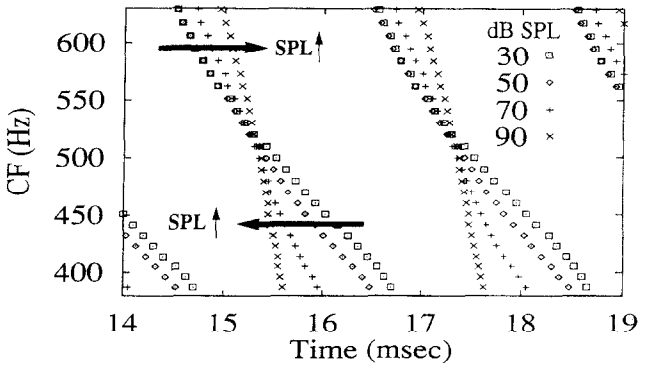

Fig. 5. Comparison of model spatio-temporal response patterns to a 500-Hz tone presented at four different SPLs. Symbols represent the times of peak probability of discharge, as illustrated in Fig. 4. A small (5 ms) segment of the spatio-temporal pattern is shown in order to highlight the changes in discharge times as a function of SPL and CF.

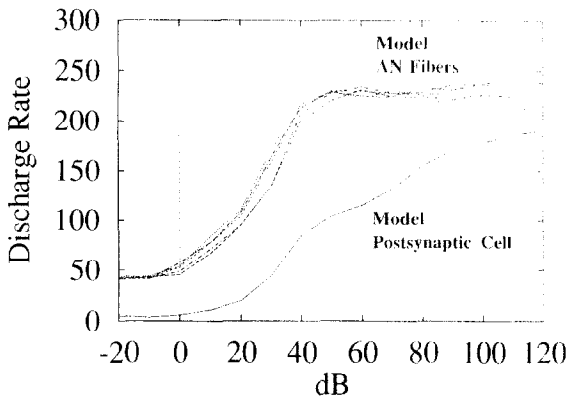

Fig. 7. Rate-level functions for 5 model AN inputs and for the model postsynaptic cell. The stimulus was a 500-Hz tone, varying over a wide range of SPL in 10 dB increments. Discharge rate is in spikes/sec. The 5 AN inputs had the following CFs: 435, 467, 500, 534, 569 Hz. Each input elicited a decaying EPSP with a 200 μs time constant. The amplitude of each input was 0.65 of the model cell's threshold. Responses are based on the average sustained rate from a simulation of 400 repetitions of a 50 ms tone presented every 100 ms.

changes illustrated above (Figs. 4 and 5). These changes were adequate to yield a wide dynamic range in the model postsynaptic cell. As level increased, the discharge times for fibers with different CFs continued to become more coincident, and thus provided an increasingly effective input to the coincidence-detecting model cell.

The dynamic range of the model postsynaptic cell is influenced by several parameters of the inputs and of the coincidence detection mechanism. In general, the responses of the model cell changed as one would

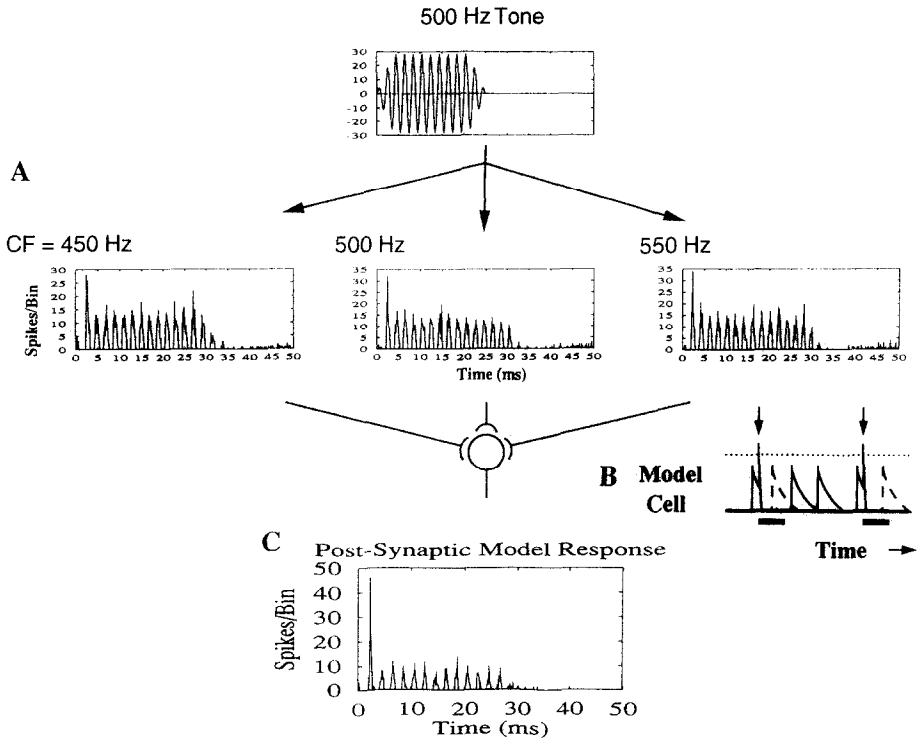

Fig. 6. Schematic diagram of the coincidence detecting cell model. A single stimulus waveform (top) serves as the input to several model AN fibers (A). On a trial by trial basis, spike times for each model AN fiber are used as inputs to the postsynaptic cell model. A schematic drawing of the postsynaptic cell's response during one such trial is shown in B. Each input spike elicits an exponentially decaying EPSP; single EPSPs are subthreshold (threshold is indicated by the horizontal dotted line). When two inputs summate to bring the cell voltage above threshold, an output spike is recorded (arrows), the cell voltage is reset to zero, and a absolute refractory period is imposed (bar below axis, see text for details). Inputs arriving during the refractory period are ineffective (dotted EPSP waveforms), and have no influence on the cell voltage. C) response of the model postsynaptic cell to the inputs shown in A.

expect from a qualitative consideration of the parameters. For example, as the time constant of decay of the input EPSPs was lengthened, the sensitivity of the cell to coincidence decreased because temporal summation of the inputs increased; this manipulation resulted in a decrease in the dynamic range of the postsynaptic cell (Fig. 8a). Similarly, as the EPSP amplitudes were increased, the requirement for coincidence decreased, and the sensitivity of the model postsynaptic cell to the changes in phase of its inputs decreases (Fig. 8b). As the range of CFs of the converging input fibers was

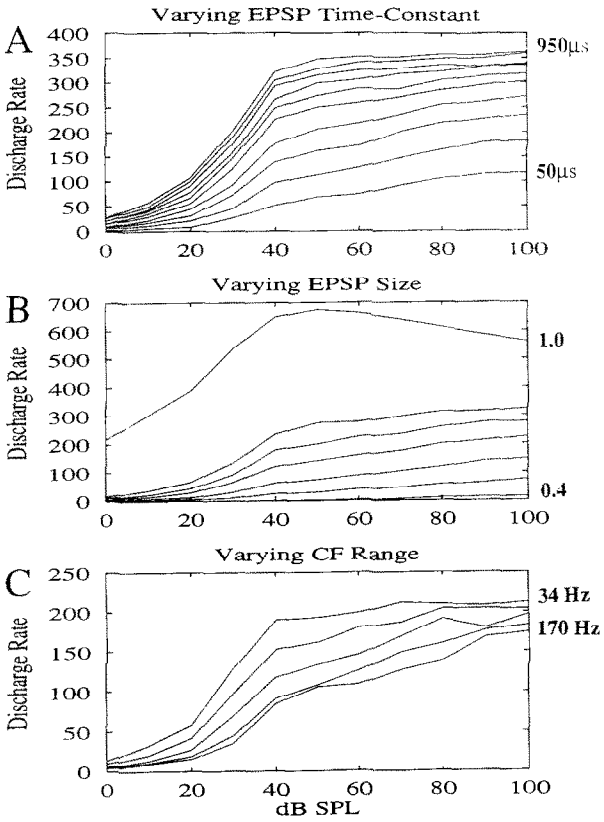

Fig. 8. Rate-level functions for the postsynaptic model cell in response to 500-Hz tones. Each panel shows rate-level functions that represent responses for several values of a given parameter, with the other model parameters held fixed. In all simulations, there were 5 model AN inputs, and the responses were to 200 repetitions of a stimulus 50 ms in duration, presented every 100 ms. The two extreme values of the variable parameter are indicated at the right of each plot. A) Each curve represents responses for a different value of the EPSP time constant, which ranged from 50 to 950 μs in increments of 100 μs. The EPSP amplitude was 0.65 of the cell's threshold, and the range of CFs was 135 Hz, centered at 500 Hz. B) Each curve represents responses for a different EPSP amplitude, which ranged from 0.4 to 1.0 relative to the cell's threshold, in increments of 0.1. The EPSP time constant was 200 μs, and the range of CFs converging on the cell was 135 Hz, centered at 500 Hz. C) Each curve represents the responses for different ranges of CFs (centered at 500 Hz) converging upon the postsynaptic model cell. The range of CFs varied from 34 Hz to 170 Hz; these ranges represent lengths along the basilar membrane that varied from 50 to 250 μm in increments of 50 μm. The EPSP time constant was 200 μs, and the EPSP amplitude was 0.65 of the cell's threshold.

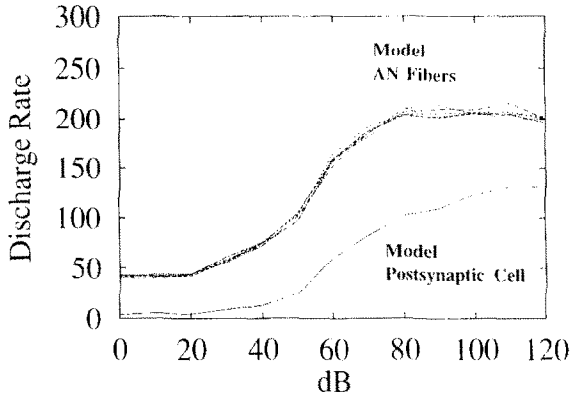

Fig. 9. Rate-level function in response to wide-band noise of the cell with the same model parameters and the same AN input CFs as in Fig. 7. Responses represent simulations of 100 repetitions of the wideband noise stimulus that was 150 ms in duration, presented every 200 ms.

increased, the absolute size of the phase cues increased (see Fig. 5) and the dynamic range of the postsynaptic cell increased (Fig. 8c). Finally, this mechanism depends upon phase-locking of the input fibers to the tones at CF; as the CF of the center fiber in the population is increased, the ability of this mechanism to provide a wide dynamic range in the postsynaptic cell decreases for responses to tones (not shown).

The mechanisms that influence the responses of low-CF fibers to tones also affect responses to complex sounds, such as noise. Low-CF fibers phase-lock to the components of a noise stimulus near the fiber's CF, and the phases of their responses are influenced by level because of the changes in the peripheral filter properties. Fig. 9 shows the rate-level functions of a post-synaptic model cell to wideband noise. Again, the dynamic range of the coincidence-detecting model cell is greater than that of the AN inputs due to the increased coincidence of the responses of fibers with different CFs as level is increased.

A model for recruitment of loudness

Given the dependence of the proposed sound level encoding scheme upon the compressive nonlinearity, it is interesting to consider the properties of the model responses when this nonlinearity is removed. This question is motivated by the evidence for the fragility of the compressive nonlinearity and by the association of its loss with sensorineural hearing impairment, and of sensorineural hearing impairment with recruitment of loudness.

Loss of the compressive nonlinearity removes the spatiotemporal cues that are necessary for this encoding scheme. This loss was simulated by removing the nonlinear feedback path from the AN model (Carney, 1993a); the 'impaired' model AN fibers had no changes in bandwidth as a function of level. Their bandwidths

were fixed and were relatively broad, as is the case for psychophysically measured filters in the hearing impaired (Dreschler and Festen, 1986; Horst, 1987; Peters and Moore, 1992); the bandwidth of the impaired model filters was set to that of normal filters at high levels, at which the nonlinear feedback is saturated and the system behaves linearly (Carney, 1993a). The broad tuning of the impaired fibers resulted in spatiotemporal response patterns that were most similar to those of the normal model in response to stimuli at high levels. Therefore, the degree of coincidence of the AN responses across CF was fixed for all levels, and was similar to the degree of coincidence in the responses of the normal model at high levels (Fig. 5).

Fig. 10 compares the responses of a coincidence detecting cell that received normal (Fig. 10a) and impaired (Fig. 10b) model AN inputs. As shown above, the normal model had a wide dynamic range because the inputs became progressively more coincident as level was increased. The rate-level function of the impaired model had an increase slope and a relatively narrow dynamic range; its inputs were well correlated at relatively low levels and therefore were more effective in driving the postsynaptic model cell. The dynamic range of the impaired model was simply determined by that of the input fibers. Note that in order to allow direct comparison between the normal and impaired models, no threshold shift was introduced in the impaired model. A more complete model for impairment would include a threshold shift; this comparison allows the illustration of what damage to the nonlinear temporal response properties alone could contribute.

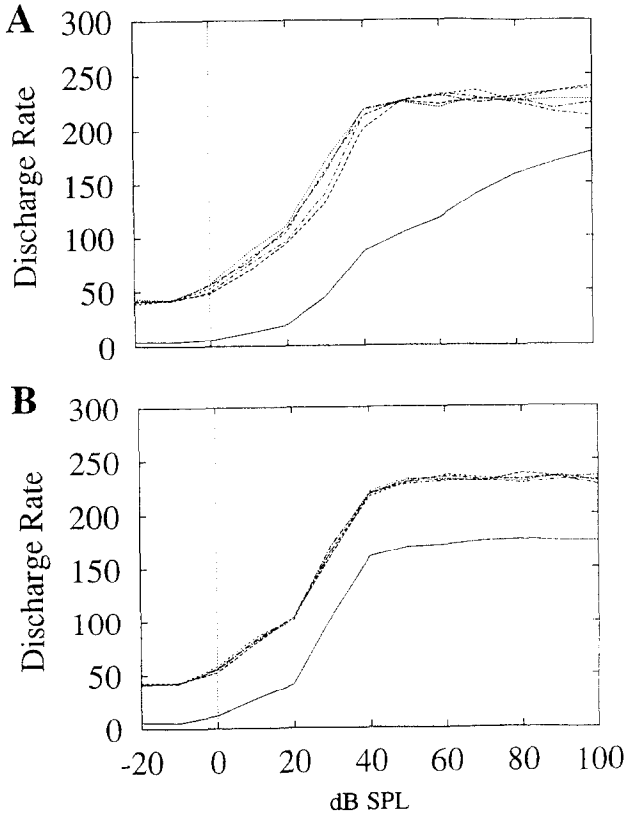

Fig. 10. A) Rate-level functions in response to 500-Hz tones of a postsynaptic cell (solid line; same model and input parameters as in Fig. 7) that receives 5 normal AN model inputs (dashed lines). B) Rate-level functions for the same model cell (solid line) that receives 5 impaired AN model inputs (dashed lines).

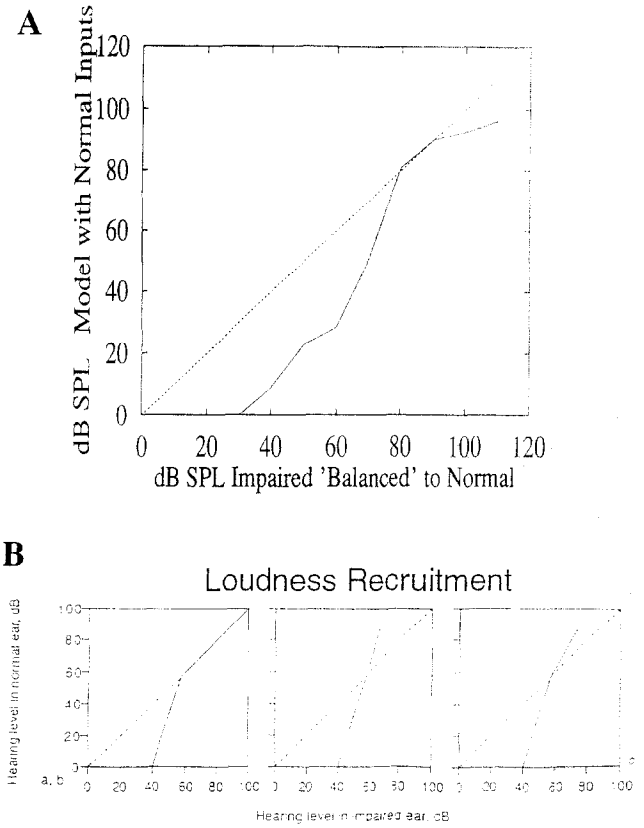

Fig. 11. A) Loudness balance function derived from the impaired and normal model responses shown in Fig. 10. The abscissa of each point on the balance function is determined by the sound level of the stimulus presented to the impaired model; the discharge rate of the impaired model in response to that stimulus is used to determine the ordinate by finding the sound level that would have produced the same discharge rate for the normal model. The dashed line shows a normal loudness balance function. For this illustration, a 40-dB increase in threshold was added to the impaired model (see text). B) Illustration of different forms of recruitment reported by Hood (1977, reprinted with permission).

Fig. 11a is a loudness balance curve derived from the responses of the model cells shown in Fig. 10. Each point along the abscissa represents the sound level presented to the impaired model; the value of the ordinate for each point was determined by finding the sound level for the normal model that would have produced a discharge rate that corresponded to that produced by the impaired model. In this case, a 40-dB threshold shift was included in the impaired model for the sake of comparison with loudness balance curves reported as evidence for different forms of recruitment

of loudness (Fig. 11b; from Hood, 1977). Each panel in this figure shows a variation of the fundamental phenomenon of loudness recruitment, the increase in growth of loudness of the impaired ear with respect to the normal ear over some range of SPLs. If the responses of the coincidence-detecting cell are interpreted in terms of the perception of loudness, then the reduced dynamic range for perceived loudness experienced with many forms of sensorineural impairment is consistent with the properties of this encoding scheme.

4. Discussion

This study has presented the hypothesis that spatiotemporal cues play a role in the encoding of sound level. Coincidence detection across AN fibers with different CFs was tested as a neural mechanism for decoding this cue. This encoding scheme is particularly attractive at low CFs, where the spatiotemporal patterns provide a robust representation of level, and convergence of a few fibers is sufficient to produce a postsynaptic neuron with a wide dynamic range. The model cell used to decode the spatiotemporal cue is very simple. However, similar coincidence-detecting properties can be obtained with a model that includes the biophysical properties of globular bushy cells in the AVCN (Stutman and Carney, 1993).

High-CF responses

It is also interesting to consider the potential role of spatiotemporal patterns and coincidence detection at higher CFs. Due to limitations in the AN model used here (Carney, 1993a), which was explicitly developed to study low-CF responses, high-CF responses were not simulated in this study. However, we can consider the implications of spatiotemporal patterns and a coincidence mechanism for encoding of level at high CFs. AN fibers with high CFs do not phaselock to the fine structure of pure tone stimuli. In response to complex stimuli, however, there are spatiotemporal cues in the responses of high-CF fibers. The responses of high-CF fibers with neighboring CFs are correlated to each other if the peripheral filters governing their responses overlap in frequency. This correlation is introduced by the fact that high-CF fibers phase-lock to the envelope of a modulated signal (e.g. Joris and Yin, 1992), and the narrowband filtering of complex sounds by the periphery produces signals with envelope modulations. Young and Sachs (1989) demonstrated such correlation between responses to wideband noise of high-CF AN fibers with neighboring CFs.

The correlation between neighboring high-CF fibers should change systematically as a function of level. As level increases, and the bandwidths of the peripheral filters increase due to the compressive nonlinearity, the overlap in frequency between neighboring filters increases, as shown schematically in Fig. 12. The increased overlap should result in increased correlation between the responses of the fibers. The same postsynaptic mechanism of coincidence detection, which is effectively cross-correlation (e.g. Yin et al., 1987), is appropriate to decode this cue for both low-CF and high-CF fibers. Such a mechanism would be limited at high levels because the AN fibers do not phase-lock to the envelopes of modulated stimuli at high levels (Smith and Brachman, 1980b; Joris and Yin, 1992) presumably due to saturation of the inner hair cell responses.

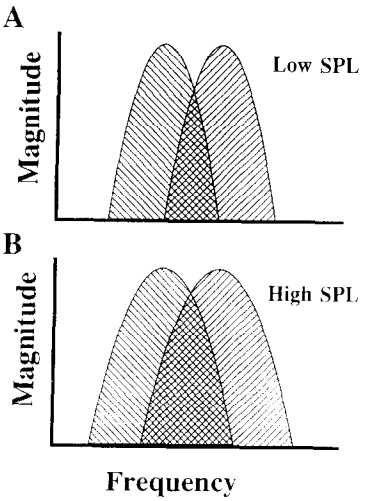

Fig. 12. Schematic illustration of the effect of a change in the bandwidth as a function of SPL on the overlap, and thus correlation, of neighboring peripheral filters.

In response to high-frequency tones presented in quiet, there is presumably no information in the spatiotemporal patterns that could encode the level over a wide dynamic range because high-CF fibers do not phase-lock to tones with frequencies near CF, and no envelope information is available for a pure tone. Rate cues that could encode sound level for high-frequency tones are spread of excitation (e.g. Siebert, 1965; Florentine and Buus, 1981; Delgutte, 1987) and contributions of non-saturating high-frequency AN fibers (Delgutte, 1987; Winslow et al., 1987; Viemeister, 1988a,b; Winter and Palmer, 1991). The use of these rate-related cues for tones and the use of spatiotemporal cues for complex sounds are not mutually exclusive mechanisms; in fact, a coincidence-detecting cell that receives convergent input from fibers with different CFs could decode the spread of excitation cue because the probability of coincident inputs would increase as the number of excited inputs to the cell increased.

Anatomical and physiological correlates

The requirements of the postsynaptic model cell are consistent with any cells that receive convergent, subthreshold inputs from primary afferents with different

CFs. For example, globular bushy cells in the AVCN receive convergent inputs from AN fibers (Osen, 1969, 1970; Lorente de Nó, 1981) and are candidates for decoding peripheral cues related to level due to their projection to the lateral superior olive (LSO), via the medial nucleus of the trapezoid body (MNTB). Medium-to-high CF 'E/I' cells in the LSO are sensitive to interaural level differences (ILDs); the dominant inputs to these cells are excitation from the ipsilateral spherical bushy cells, and contralateral inhibition from the globular bushy cells, via the MNTB (Warr, 1982). Responses of MNTB neurons follow their inputs in a one-to-one fashion (Guinan and Li, 1990) and thus preserve the information of their globular bushy cell inputs. In order for LSO cells to be sensitive to ILDs across a wide range of mean binaural levels (e.g. Boudreau and Tsuchitani, 1968; Goldberg and Brown, 1969; Tsutchitani, 1977; Caird and Klinke, 1983), either one of their inputs must exhibit a wide dynamic range, or they must themselves process convergence inputs with a range of different CFs.

Other cell types in the cochlear nucleus are also candidates for processing of spatiotemporal information related to sound level. For example, onset chopper response types in the ventral cochlear nucleus, which are known to receive convergent inputs from a wide tonotopic region of the auditory nerve root and to have wide dynamic ranges (Smith and Rhode, 1989), may act as coincidence detectors (Palmer and Winter, 1993). Other types of onset units have also been reported to have wide-dynamic ranges (Bourk, 1976; Frisina et al., 1990). Onset cells were among those shown to be sensitive to changes in the spatiotemporal patterns of their inputs (Carney, 1990), a property consistent with their acting as coincidence detectors. Different types of onset cells may play a role in encoding of level; however, based on the patterns of their anatomical projections (Warr, 1982) they are presumably not involved in the analysis of interaural level differences that takes place in the LSO.

A simple preservation of the dynamic range present in peripheral fibers could be accomplished only if the postsynaptic cells received a single suprathreshold input, and discharged in a one-to-one fashion. In the AVCN, this synaptic arrangement is only apparent for spherical bushy cells (Pfeiffer, 1966; Bourk, 1976). If the inputs to the cells are subthreshold, then the correlation between those inputs becomes important in determining the discharge probability of the postsynaptic cell, and peripheral nonlinearities that affect timing must be considered. These issues are particularly relevant for globular bushy cells that have nonlinear membrane properties that reduce temporal summation of their inputs (Oertel, 1983), thus making them more sensitive to the coincidence of their inputs (Carney, 1990; Manis and Marx, 1991). The fact that spontaneous rates of these neurons are generally low also suggests that a mechanism such as coincidence detection plays a role in their response properties. Although high spontaneous rates are occasionally seen, the majority of AVCN cells with responses characteristic of globular bushy cells (i.e. primarylike-with-notch and onset-with-low-sustained-activity PST histograms in response to tones) have relatively low spontaneous rates (Blackburn and Sachs, 1989; Smith et al., 1991), despite the fact that they receive convergent AN inputs (Osen, 1969, 1970; Lorente de Nó, 1981) that are predominantly high-spontaneous rate fibers (Liberman, 1991).

Comparison with other models

Other models that process spatiotemporal information have been proposed; however, there are significant differences between the mechanisms that are exploited by each of these models and the one presented here. Deng and Geisler (1987) proposed a composite model that analyzed spatiotemporal patterns in response to speech stimuli. They proposed an algorithm for detection of formant frequencies that involved cross-correlation across neighboring AN fibers; formants were indicated by a reduction in the value of the correlation coefficient, due to abrupt changes in the spatiotemporal pattern. Although their AN model included nonlinearities that influenced the 'capture' of synchrony across fibers of different CF, it is not clear that the fine timing of the spatiotemporal patterns varied as a function of level (results were only illustrated for one SPL). Based on the empirical evidence for changes in phase as a function of level, the correlation coefficient they measured should increase with increasing level, thus reducing the detectability of formants at high levels based upon a decrease in the correlation coefficient.

Shamma (1985) also proposed a mechanism for detection of spectral peaks based on spatiotemporal patterns of AN responses coupled with a lateral inhibitory network (LIN). The LIN served to enhance discontinuities in the spatiotemporal discharge pattern, and thus was intended to detect spectral peaks that are expected to elicit rapid phase transitions across groups of fibers. Again, the size of this cue changes with level due to the nonlinear temporal response properties of the AN. As level increases, the discontinuity in the spatiotemporal pattern associated with a spectral peak is reduced, and thus the performance of the LIN should be reduced at higher levels.

The model presented here provides a relatively simple scheme, compared to the above models, by taking advantage of the peripheral nonlinearity that influences spatiotemporal patterns. This model requires the simplest form of a cross-correlation mechanism: the correlation is performed at only one time delay (that fixed by the delays leading to the postsynaptic cell), unlike the correlation coefficient function, which is

performed at many different delays, and then followed by a minimum detector (Deng and Geisler, 1987). Also, the model only requires the mechanism of a coincidence detector acting on excitatory inputs, for which there is evidence in the AVCN, rather than the more sophisticated circuitry required by the LIN model.

Recruitment of loudness

The potential role of spatiotemporal cues for encoding level, and thus the involvement in the perception of loudness, suggests that we consider the possible contribution of impairment of this mechanism to the phenomenon of recruitment of loudness. Indeed, the nature of the spatiotemporal encoding of level, and the properties of a postsynaptic coincidence detector, suggest a specific manner in which the loss of the peripheral nonlinearity could contribute to recruitment. If we assume that the CNS uses the proposed scheme for processing normal spatiotemporal patterns to decode level and determine loudness, then the same processing scheme, when applied to impaired inputs, would yield recruitment.

A previous model for recruitment was proposed on the basis of physiological experiments in animals that were treated with kanamycin to induce sensorineural impairment (Kiang et al., 1970). That study concluded that there was no difference in the slopes of rate-level functions for acoustically-stimulated AN fibers in the impaired animals. However, there was a notable increase in the number of high-threshold fibers with CFs near the border of the most impaired region of the cochlea. It was concluded that the increased number of fibers with CFs in this range could explain recruitment, for, as the sound level of a stimulus is raised, an increased number of fibers would be 'recruited'. More recent studies of AN tuning in ears that were acoustically traumatized would suggest that the abundant 'low-CF' fibers were actually the remaining 'tails' of tuning curves of high-CF fibers for which the sensitive 'tips' were lost (e.g. Liberman and Dodds, 1987). If this is the case, then there is no increase in the number of fibers that would response to a stimulus of a particular frequency after sensorineural impairment; the same high-CF fibers would presumably have responded to high-level stimuli presented at a frequency in their 'tails' before the impairment.

The model described here has interesting implications for a special case of recruitment. Patients with cochlear implants are reported to have a comfortable dynamic range of only 10–20 dB (Shannon, 1993). Electrically stimulated AN fibers are known to exhibit exceptionally strong phase-locking (e.g. Kiang and Moxon, 1972; Van den Honert and Stypulkowski, 1987; Dynes and Delgutte, 1992), and groups of fibers that are stimulated by the same electrode will presumably all fire in synchrony. Such highly synchronized input would provide unnaturally effective inputs to a postsynaptic cell that was performing coincidence detection upon its converging inputs. Thus, the very limited dynamic range of cochlear implant patients may be partly explained by a coincidence detection mechanism that receives the unnatural spatiotemporal patterns elicited by electrical stimulation. Other mechanisms probably contribute to recruitment in the case of electrical stimulation as well. For example, in some cases the rate-level functions of electrically stimulated AN fibers are very steep, and thus mechanisms that use rate cues could also produce recruitment of loudness.

Limitations of the model & future directions

The simulations presented here are limited in several respects. First, inaccuracies in the temporal response properties of the AN model will influence the responses of the model coincidence-detecting cell. Limitation of the AN model to low-CF fibers prevents the extension of testing at high frequencies of the hypothesis presented here. Further study of the nonlinear temporal properties of AN fibers will be necessary in order to develop a more general AN model. Another limitation of the model is the simple shot-noise model for the postsynaptic cell. This model requires 'EPSPs' that are unphysiologically short in duration in order to provide reasonably sensitive coincidence detection. In future work, this model might be replaced with a more physiological model for coincidence detecting neurons that has been recently developed (Stutman and Carney, 1993); however, the more physiologically realistic model introduces higher computational demands. In addition, the coincidence model assumed equal neural delays between each AN fiber and the postsynaptic cell. More realistic neural delays for the different inputs to postsynaptic cells can only be determined with future physiological experiments designed to measure the spatiotemporal tuning of these cells.

The hypothesis for encoding of level presented here can be further explored with psychophysical experiments that test the role of spatiotemporal patterns in the perception of loudness in normal ears. Specifically, the mean and variance of the postsynaptic discharge rates can be compared to those of the AN inputs and to psychophysically derived estimates of intensity jnds and loudness growth functions. Psychophysical manipulation of the perception of loudness by manipulation of spatiotemporal cues would also provide evidence for the proposed hypothesis. Also, the potential for manipulating the spatiotemporal patterns by manipulating phase cues is suggested as a possible strategy to at least partially reverse the phenomenon of recruitment of loudness in impaired ears. Such a strategy would complement efforts to compensate for recruitment using amplification with automatic gain control (e.g. Moore and Glasberg, 1988; Rankovic et al., 1992).

Acknowledgements

I would like to especially thank Ajit Janardhan for his assistance in running computer simulations. Many of my colleagues provided helpful remarks on earlier versions of this manuscript; thanks to D.A. Cameron, H.S. Colburn, A. Cure, B. Delgutte, R.A. Eatock, M. Friedman, R. Hellman, W. Hellman, P.X. Joris, G. Kidd, P.H. Smith, E. Stutman, and J. Tracy. This work was supported by a grant from the Whitaker Foundation and by NIH grant No. 1 R29 DC01641-01.

References

Anderson, D.J., Rose, J.E., Hind, J.E. and Brugge, J.F. (1971) Temporal position of discharges in single auditory nerve fibers within the cycle of a sine-wave stimulus: Frequency and intensity effects. J. Acoust. Soc. Am. 49, 1131–1139.

Blackburn, C.C. and Sachs, M.B. (1989) Classification of unit types in the anteroventral cochlear nucleus: PST histograms and regularity. J. Neurophysiol. 62, 1303–1329.

Boudreau, J.C. and Tsuchitani, C. (1968) Binaural interactions in cat superior olive S-segment. J. Neurophysiol. 31, 442–454.

Bourk, T.R. (1976) Electrical Responses of Neural Units in the Anteroventral Cochlear Nucleus of the Cat (PhD dissertation). Cambridge, MA.

Caird, D. and Klinke, R. (1983) Processing of binaural stimuli by cat superior olivary complex neurons. Exp. Brain. Res. 52, 385–399.

Carney, L.H. (1990) Sensitivities of cells in the anteroventral cochlear nucleus of cat to spatiotemporal discharge patterns across primary afferents. J. Neurophysiol. 437–456.

Carney, L.H. (1992) Modelling the sensitivity of cells in the anteroventral cochlear nucleus to spatiotemporal discharge patterns. Phil. Trans. R. Soc. Lond. B 336, 403–406.

Carney, L.H. (1993a) A model for the responses of low-frequency auditory-nerve fibers in cat. J. Acoust. Soc. Am. 93, 401–417.

Carney, L.H. (1993b) A model for spatio-temporal encoding of sound pressure level: Effect of the compressive nonlinearity. Abstr. Assoc. Res. Otolaryngol. 16, 79.

Carney, L.H. and Yin, T.C.T. (1988) Temporal coding of resonances by low-frequency auditory nerve fibers: Single fiber responses and a population model. J. Neurophysiol. 60, 1653–1677.

Colburn, H.S. (1984) Models of intensity discrimination. J. Acoust. Soc. Am. 76, S5.

Colburn, H.S., Han, Y-A. and Culotta, C.P. (1990) Coincidence model of MSO responses. Hear. Res. 49, 335–346.

Delgutte, B. (1987) Peripheral processing of speech information: Implications from a physiological study of intensity discrimination. In: M.E.H. Schouten (Ed.), Psychophysics and Speech Perception, Nijhoff, Dordrecht, the Netherlands, pp. 333–353.

Deng, L. and Geisler, C.D. (1987) A composite auditory model for processing speech sounds. J. Acoust. Soc. Am. 82, 2001–2012.

Dreschler, W.A. and Festen, J.M. (1986) The effect of hearing impairment on auditory filter shapes in simultaneous and forward masking. In: B.C.J. Moore and R.D. Patterson (Eds.), Auditory Frequency Selectivity, Plenum Press, NY, pp. 331–340.

Dynes, S.B.C. and Delgutte, B. (1992) Phase-locking of auditory-nerve discharges to sinusoidal electric stimulation of the cochlea. Hear. Res. 58, 79–90.

Evans, E.F. (1978) Place and timing coding of frequency in the peripheral auditory system: Some physiological pros and cons. Audiology 17, 369–420.

Evans, E.F. (1981) The dynamic range problem: Place and timing coding at the level of the cochlear nerve and nucleus. In: J. Syka and L. Aitkin (Eds.), Neuronal Mechanisms of Hearing, Plenum Press, NY, pp. 69–85.

Evans, E.F. and Palmer, A.R. (1980) Relationship between the dynamic range of cochlear nerve fibers and their spontaneous activity. Exp. Brain Res. 40, 115–118.

Florentine, M. and Buus, S. (1981) An excitation-pattern model for intensity discrimination. J. Acoust. Soc. Am. 70, 1646–1654.

Fowler, E.P. (1936) A method for the early detection of otosclerosis. Arch. Otolaryngol. 24, 731–741.

Frisina, R.D., Smith, R.L. and Chamberlain, S.C. (1990) Encoding of amplitude modulation in the gerbil cochlear nucleus: II. Possible neural mechanisms. Hear. Res. 44, 123–142.

Goldberg and Brown (1969) Response of binaural neurons of dog superior olivary complex to dichotic tonal stimuli: some physiological mechanisms of sound localization. J. Neurophysiol. 32, 613–636.

Guinan, J.J., Jr. and Li, R.Y.-S. (1990) Signal processing in brainstem auditory neurons which receive giant endings (calyces of Held) in the medial nucleus of the trapezoid body in cat. Hear. Res. 49, 321–334.

Hellman, R.P. (1974) Effect of spread of excitation on the loudness function at 250 Hz. In: H.R. Moskowitz et al. (Eds.), Sensation and Measurement, D. Reidel Publishing Co., Dordrecht, the Netherlands, pp. 241–249.

Hellman, R.P. (1978) Dependance of loudness growth on skirts of excitation patterns. J. Acoust. Soc. Am. 63, 1114–1119.

Hood, J.D. (1969) Basic audiological requirements in neuro-otology. J. Laryngol. Otol. 83, 695–711.

Hood, J.D. (1977) Loudness balance procedures for the measurement of recruitment. Audiology 16, 215–228.

Horst, J.W. (1987) Frequency discrimination of complex signals, frequency selectivity and speech perception in hearing-impaired subjects. J. Acoust. Soc. Am. 82, 874–885.

Horst, J.W., Javel, E. and Farley, G.R. (1990) Coding of spectral fine structure in the auditory nerve II. Level-dependent nonlinear responses. J. Acoust. Soc. Am. 88, 2656–2681.

Jerger, J. (1962) Hearing tests in otological diagnosis. ASHA Rep. 4, 139–145.

Johnson, D.H. (1980) The relationship between spike rate and synchrony in responses of auditory-nerve fibers to single tones. J. Acoust. Soc. Am. 68, 1115–1122.

Joris, P.X., Carney, L.H., Smith, P.H. and Yin, T.C.T. (1994) Enhancement of neural synchronization in the anteroventral cochlear nucleus. I: Responses to tones at the characteristic frequency. J. Neurophysiol. (in press).

Joris, P.X. and Yin, T.C.T. (1992) Responses to amplitude-modulated tones in the auditory nerve of the cat. J. Acoust. Soc. Am. 91, 215–232.

Kiang, N.Y.-S. and Moxon, E.C. (1972) Physiological considerations in artificial stimulation of the inner ear. Ann. Otol. Rhinol. Laryngol. 81, 714–732.

Kiang, N.Y.-S., Moxon, E.C. and Levine, R.A.L. (1970) Auditory-nerve activity in cats with normal and abnormal cochleas. In: G.E.W. Wolstenholme and J. Knight (Eds.), Sensorineural Hearing Loss, Ciba Symposium, J. and A. Churchill, London, pp. 241–273.

Kiang, N.Y.-S., Watanabe, T., Thomas, E.C. and Clark, L.F. (1965) Discharge patterns of single fibers in the cat's auditory nerve. MIT Research Monograph No. 35. M.I.T. Press, Cambridge, MA.

Lai, Y.C., Winslow, R.L. and Sachs, M.B. (1993) Selective processing of auditory-nerve inputs by AVCN chopper cells. Abstr. Assoc. Res. Otolaryngol. 16, 121.

Liberman, M.C. (1978) Auditory-nerve response from cats raised in a low-noise chamber. J. Acoust. Soc. Am. 63, 442–455.

Liberman, M.C. (1991) Central projections of auditory-nerve fibers

of differing spontaneous rate. I. Anteroventral cochlear nucleus. J. Comp. Neurol. 313, 240–258.
Liberman, M.C. and Dodds, L.W. (1987) Acute ultrastructural changes in acoustic trauma: Serial-section reconstruction of stereocilia and cuticular plates. Hear. Res. 26, 45–64.
Lorente de Nó, R. (1981) The Primary Acoustic Nuclei. Raven Press, NY.
Manis, P.B. and Marx, S.O. (1991) Outward currents in isolated ventral cochlear nucleus neurons. J. Neurosci. 11, 2865–2880.
May, B.J. and Sachs, M.B. (1992) Dynamic range of neural rate responses in the ventral cochlear nucleus of awake cats. J. Neurophysiol. 68, 1589–1602.
Moore, B.C.J. (1989) An Introduction to the Psychology of Hearing, 3rd edition. Academic Press, NY, 350 pp.
Moore, B.C.J. and Glasberg, B.R. (1987) Formulae describing frequency selectivity as a function of frequency and level, and their use in calculating excitation patterns. Hear. Res. 28, 209–225.
Moore, B.C.J. and Glasberg, B.R. (1988) A comparison of our methods of implementing automatic gain control (AGC) in hearing aids. Br. J. Audiol. 22, 93–104.
Moore, B.C.J., Glasberg, B.R., Hess, R.F. and Birchall, J.P. (1985) Effects of flanking noise bands on the rate of growth of loudness of tones in normal and recruiting ears. J. Acoust. Soc. Am. 77, 1505–1513.
Oertel, D.O. (1983) Synaptic responses and electrical properties of cells in brain slices of the mouse anteroventral cochlear nucleus. J. Neurophysiol. 3, 2043–2053.
Osen, K.K. (1969) The intrinsic organization of the cochlear nuclei in the cat. Acta Oto. Laryngolog. 67, 352–359.
Osen, K.K. (1970) Course and terminations of the primary afferents in the cochlear nuclei of the cat. An experimental study. Arch. Ital. Biol. 108, 21–51.
Palmer, A.R. (1982) Encoding of rapid amplitude fluctuations by cochlear-nerve fibres in the guinea-pig. Arch. Otorhinolaryngol. 236, 197–202.
Palmer, A.R. and Evans, E.F. (1982) Intensity coding in the auditory periphery of the cat: Responses of cochlear nerve and cochlear nucleus neurons to signals in the presence of bandstop masking noise. Hear. Res. 7, 305–323.
Palmer, A.R. and Winter, I.M. (1993) Best-frequency (BF) threshold reductions caused by off-BF non-excitatory tones in onset units of the cochlear nucleus. Abstr. Assoc. Res. Otolaryngol. 16, 123.
Patuzzi, R. and Robertson, D. (1988) Tuning in the mammalian cochlea. Physiolog. Rev. 68, 1009–1082.
Patuzzi, R.B., Yates, G.K. and Johnstone, B.M. (1989) Changes in cochlear microphonic and neural sensitivity produced by acoustic trauma. Hear. Res. 39, 189–202.
Peters, R.W. and Moore, B.C.J. (1992) Auditory filter shapes at low center frequencies in young and elderly hearing-impaired subjects. J. Acoust. Soc. 91, 256–266.
Pick, G.F. (1980) Level dependence of psychophysical frequency resolution and auditory filter shape. J. Acoust. Soc. Am. 68, 1085–1095.
Pfeiffer, R.R. (1966) Anteroventral cochlear nucleus: wave forms of extracellularly recorded spike potentials. Science Washington, DC 154, 667–668.
Rankovic, C.M., Freyman, R.L. and Zurek, P.M. (1992) Potential benefits of adaptive frequency-gain characteristics for speech reception in noise. J. Acoust. Soc. Am. 91, 354–362.
Rhode, W.S. (1971) Observations of the vibration of the basilar membrane using the Mossbauer technique. J. Acoust. Soc. Am. 49, 1218–1231.
Robles, L., Ruggero, M.A. and Rich, N.C. (1986) Basilar membrane mechanics at the base of the chinchilla cochlea. I. Input-output functions, tuning curves, and phase responses. J. Acoust. Soc. Am. 80, 1364–1374.
Ruggero, M.A. (1992) Responses to sound of the basilar membrane of the mammalian cochlea. Curr. Opinion Neurobiol. 2, 449–456.
Ruggero, M.A. and Rich, N.C. (1991) Furosemide alters organ of corti mechanics: Evidence for feedback of outer hair cells upon the basilar membrane. J. Neurosci. 11, 1057–1067.
Ruggero, M.A., Rich, N.C. and Recio, A. (1993) Acoustic overstimulation reduces basilar membrane responses to sound. Abstr. Assoc. Res. Otolaryngol. 16, 31.
Ruggero, M.A., Robles, L. and Rich, N.C. (1992) Two-tone suppression in the basilar membrane of the cochlea: Mechanical basis of auditory-nerve rate suppression. J. Neurophysiol. 68, 1087–1099.
Sachs, M.B. and Abbas, P.J. (1974) Rate versus level functions for auditory nerve fibers in cat: Tone-burst stimuli. J. Acoust. Soc. Am. 56, 1835–1847.
Sachs, M.B., Young, E.D., Winslow, R.L. and Shofner, W.P. (1986) Some aspects of rate coding in the auditory nerve. In: B.C.J. Moore and R.D. Patterson (Eds.), Auditory Frequency Selectivity, Plenum Press, NY, pp. 121–128.
Shamma, S.A. (1985) Speech processing in the auditory system II: Lateral inhibition and the central processing of speech evoked activity in the auditory nerve. J. Acoust. Soc. Am. 78, 1622–1632.
Shannon, R.V. (1993) Psychophysics. In: R.S. Tyler (Ed.), Cochlear Implants: Audiological Foundations, Singular, San Diego, CA, pp.357–388.
Siebert, W.M. (1965) Some implications of the stochastic behavior of primary auditory neurons. Kybernetik 2, 206, 215.
Smith, P.H., Joris, P.X., Carney, L.H. and Yin, T.C.T. (1991) Projections of physiologically characterized globular bushy cell axons from the cochlear nucleus of the cat. J. Comp. Neurol. 304, 387–407.
Smith, P.H. and Rhode, W.S. (1989) Structural and functional properties distinguish two types of multipolar cells in the ventral cochlear nucleus. J. Comp. Neurol. 282, 595–616.
Smith, R.L. (1988) Encoding of sound intensity by auditory neurons. In: G.M. Edelman, W.E. Gall and W.M. Cowan (Eds.), Auditory Function: Neurobiological Bases of Hearing, John Wiley and Sons, NY, pp. 243–274.
Smith, R.L. and Brachman, M.L. (1980a) Operating range and maximum response of single auditory nerve fibres. Brain Res. 184, 499–505.
Smith, R.L. and Brachman, M.L. (1980b) Response modulation of auditory-nerve fibers by AM stimuli: Effects of average intensity. Hear. Res. 2, 123–133.
Smith, R.L., Frisina, R.D. and Goodman, D.A. (1983) Intensity functions and dynamic responses from the cochlea to the cochlear nucleus. In: R. Klinke and R. Hartmann (Eds.), Hearing - Physiological Bases and Psychophysics, Springer-Verlag, Berlin, pp. 112–117.
Stutman, E.R. and Carney, L.H. (1993) A model for temporal sensitivity of cells in the auditory brainstem: The role of a slow, low-threshold potassium conductance. Abstr. Assoc. Res. Otolaryngol. 16, 121.
Tsutchitani, C. (1977) Functional organization of lateral cell groups of cat superior olivary complex. J. Neurophysiol. 40, 296–318.
Van den Honert, C. and Stypulkowski, P.H. (1987) Temporal response patterns of single auditory-nerve fibers elicited by periodic electrical stimuli. Hear. Res. 29, 207–222.
Viemeister, N.F. (1983) Auditory intensity discrimination at high frequencies in the presence of noise. Science 221, 1206–1208.
Viemeister, N.F. (1988a) Intensity coding and the dynamic range problem. Hear. Res. 34, 267–274.
Viemeister, N.F. (1988b) Psychophysical aspects of auditory intensity coding. In: G.M. Edelman, W.E. Gall and W.M. Cowan (Eds.), Auditory Function: Neurobiological Bases of Hearing, Wiley, NY, pp. 213–241.
Warr, W.B. (1982) Parallel ascending pathways from the cochlear:

Neuroanatomical evidence of functional specification. In: Contributions to Sensory Physiology. Vol 7, Academic Press, pp.1–38.

Westerman, L.A. and Smith, R.L. (1988) A diffusion model of the transient response of the cochlear inner hair cell synapse. J. Acoust. Soc. Am. 83, 2266–2276.

Winslow, R.L., Barta, P.E. and Sachs, M.B. (1987) Rate coding in the auditory nerve. In: W.A. Yost and C.S. Watson (Eds.), Auditory Processing of Complex Sounds, Erlbaum, Hillsdale, NJ, pp. 212–224.

Winslow, R.L. and Sachs, M.B. (1988) Single-tone intensity discrimination based on auditory-nerve rate responses in backgrounds of quiet, noise and with stimulation of the crossed olivocochlear bundle. Hear. Res. 35, 165–190.

Winter, I.M. and Palmer, A.R. (1991) Intensity coding in low-frequency auditory-nerve fibers of the guinea pig. J. Acoust. Soc. Am. 90, 1958–1967.

Winter, I.M., Robertson, D. and Yates, G.K. (1990) Diversity of characteristic frequency rate-intensity functions in guinea pig auditory-nerve fibers. Hear. Res. 45, 191–202.

Yates, G.K., Winter, I.M. and Robertson, D. (1990) Basilar membrane nonlinearity determines auditory nerve rate-intensity functions and cochlear dynamic range. Hear. Res. 45, 203–220.

Yin, T.C.T., Chan, J.C.K. and Carney, L.H. (1987) Effects of interaural time delays of noise stimuli on low-frequency cells in the cat's inferior colliculus. III. Evidence for cross-correlation. J. Neurophysiol. 58, 562–583.

Young, E.D., Rothman, J.S. and Manis, P.B. (1993) Regularity of discharge constrains models of ventral cochlear nucleus bushy cells. In: M. Merchen and J. Juiz (Eds.), The Mammalian Cochlear Nuclei: Organization and Function, Plenum Press, NY, pp. 395–410.

Young, E.D. and Sachs, M.B. (1979) Representation of steady-state vowels in the temporal aspects of the discharge patterns of auditory-nerve fibers. J. Acoust. Soc. Am. 66, 1381–1403.

Young, E.D. and Sachs, M.B. (1989) Auditory nerve fibers do not discharge independently when responding to broadband noise. Abstr. Assoc. Res. Otolaryngol. 12, 121.